

000 001 002 003 004 005 006 007 008 009 010 011 012 013 014 015 016 017 018 019 020 021 022 023 024 025 026 027 028 029 030 031 032 033 034 035 036 037 038 039 040 041 042 043 044 045 046 047 048 049 050 051 052 053 ONE-TOKEN ROLLOUT: GUIDING SUPERVISED FINE-TUNING OF LLMs WITH POLICY GRADIENT

Anonymous authors

Paper under double-blind review

ABSTRACT

Supervised fine-tuning (SFT) is the predominant method for adapting large language models (LLMs), yet it often struggles with generalization compared to reinforcement learning (RL). In this work, we posit that this performance disparity stems not just from the loss function, but from a more fundamental difference: SFT learns from a fixed, pre-collected dataset, whereas RL utilizes on-policy data sampled from the current policy. Building on this hypothesis, we introduce one-token rollout (OTR), a novel fine-tuning algorithm that guides SFT with the policy gradient method. OTR reframes the autoregressive learning process by treating each token generation as a single-step reinforcement learning trajectory. At each step, it performs a Monte Carlo “rollout” by sampling multiple candidate tokens from the current policy’s distribution. The ground-truth token from the supervised data is then used to provide a reward signal to these samples. Guided by policy gradient, our algorithm repurposes static, off-policy supervised data into a dynamic, on-policy signal at the token level, capturing the generalization benefits of on-policy learning while bypassing the costly overhead of full sentence generation. Through extensive experiments on a diverse suite of challenging benchmarks spanning mathematical reasoning, code generation, and general domain reasoning, we demonstrate that OTR consistently outperforms standard SFT. Our findings establish OTR as a powerful and practical alternative for fine-tuning LLMs and provide compelling evidence that the on-policy nature of data is a critical driver of generalization, offering a promising new direction for fine-tuning LLMs.

1 INTRODUCTION

Supervised fine-tuning (SFT) has become a cornerstone for adapting large language models (LLMs) to downstream tasks (Ouyang et al., 2022; Chung et al., 2022; Zhang et al., 2025). However, a growing body of evidence suggests that while SFT excels at mimicking expert demonstrations, it often struggles with generalization compared to methods based on reinforcement learning (RL) (Chu et al., 2025a; Huan et al., 2025; Shenfeld et al., 2025). Recent research Chu et al. (2025a) has proposed the view that “SFT memorizes, while RL generalizes”. This limitation is particularly concerning as SFT can disrupt the well-formed distributions learned during pre-training, leading to a degradation of general capabilities—a phenomenon sometimes referred to as catastrophic forgetting (Kumar et al., 2022; Huan et al., 2025; Shenfeld et al., 2025).

This generalization gap motivates a deeper investigation into the fundamental differences between SFT and RL, with the goal of enhancing the generalization of SFT by borrowing principles from RL. Recent advancements in RL have demonstrated that even simplified methods, such as GPG (Chu et al., 2025b), which directly optimize an objective structurally similar to a weighted SFT loss, can achieve performance comparable to more complex algorithms like PPO (Schulman et al., 2017) or GRPO (Shao et al., 2024). This suggests that the performance disparity between SFT and RL may not solely stem from the loss function, but also from a more fundamental difference: the nature of the data used for updates. SFT typically relies on a static, pre-collected set of expert demonstrations, which is known as off-policy data, whereas RL methods utilize on-policy data sampled iteratively from the current policy.

As RL becomes an increasingly popular paradigm for fine-tuning LLMs, the critical role of on-policy data has garnered significant attention (Tajwar et al., 2024; Ren & Sutherland, 2024; Shenfeld et al.,

054 Tajwar et al. (2024) has shown that on-policy sampling is crucial for RL to discover optimal
 055 policies, especially when the target behavior lies in low-probability regions of the initial model. It
 056 provides a more stable and effective learning signal by ensuring that policy updates are made in
 057 regions the model can already reach, thereby preventing drastic and potentially harmful shifts in
 058 the output distribution (Ren & Sutherland, 2024; Shenfeld et al., 2025). This suggests that the on-
 059 policy nature of RL is a key factor contributing to its superior generalization and ability to preserve
 060 pre-trained knowledge.

061 Inspired by these insights, we propose one-token rollout (OTR) algorithm, a novel fine-tuning
 062 method that aims to enhance the generalization of SFT from a data-centric perspective. OTR guides
 063 the fine-tuning process with the policy gradient method, treating each token-generation step as an
 064 individual, on-policy learning event. By performing a Monte Carlo “rollout” at each token position
 065 which samples candidate tokens from the current policy and using the ground-truth token as a reward
 066 signal, OTR transforms the off-policy supervised data into a token-level on-policy signal.

067 OTR enhances generalization by narrowing the data-side gap between SFT and RL, while its de-
 068 sign as a token-level method bypasses the costly generation of complete, sentence-level on-policy
 069 training data. Our extensive experiments demonstrate that this on-policy simulation consistently
 070 improves the generalization of fine-tuned models across a wide array of challenging mathematical,
 071 coding, and general reasoning benchmarks. These results not only validate the efficacy of OTR as a
 072 powerful alternative for fine-tuning LLMs but also provide strong evidence for the critical role that
 073 on-policy data plays in the generalization performance of fine-tuned language models.

074 Our contributions can be summarized as follows:
 075

- 076 • We introduce One-Token Rollout, a novel fine-tuning algorithm that guides SFT with the
 077 policy gradient method. By treating each token generation as a single-step reinforcement
 078 learning task, OTR improves model generalization without incurring the high computa-
 079 tional cost of full sentence generation.
- 080 • We provide a new data-centric perspective on the SFT-RL generalization gap, positing that
 081 the on-policy nature of training data is a critical factor. The success of our token-level
 082 on-policy simulation serves as strong evidence for this viewpoint.
- 083 • We conduct extensive experiments on a wide array of challenging benchmarks across math-
 084 ematical, coding, and general reasoning domains. Our results empirically demonstrate that
 085 OTR consistently outperforms SFT, validating its efficacy as a powerful and practical alter-
 086 native for fine-tuning LLMs.

088 2 PRELIMINARIES

091 2.1 SUPERVISED FINE-TUNING

093 The standard approach for adapting pre-trained LLMs to specific downstream tasks is Supervised
 094 Fine-Tuning. Given a dataset of prompt-response pairs, where the response X is a sequence of
 095 tokens $\{x_1, x_2, \dots, x_T\}$, SFT aims to maximize the conditional probability of the ground-truth
 096 sequence. This is typically achieved by minimizing the negative log-likelihood loss, autoregressively
 097 training the model π_θ to predict the next token x_t given the preceding context $x_{1:t-1}$:

$$099 \mathcal{L}_{\text{SFT}}(\theta) = -\frac{1}{T} \sum_{t=1}^T \log \pi_\theta(x_t | x_{1:t-1}). \quad (1)$$

102 2.2 POLICY GRADIENT

105 Policy gradient represents a class of reinforcement learning algorithms that directly optimize a pa-
 106 rameterized policy, π_θ . In this framework, the text generation process is modeled step-by-step. At
 107 each timestep t , the state s_t is the sequence of previously generated tokens $x_{1:t-1}$, and the action a_t
 is the next token selected by the policy from the vocabulary.

108 The core objective is to adjust the policy’s parameters, θ , to maximize the expected total reward.
 109 This objective function, $J(\theta)$, is defined as the expected cumulative reward:
 110

$$111 \quad J(\theta) = \mathbb{E}_{\tau \sim \pi_\theta} \left[\sum_{t=1}^T r(s_t, a_t) \right], \quad (2)$$

113 where $r(s_t, a_t)$ is the scalar reward received after taking action a_t in state s_t , and τ is the entire
 114 sequence of states and actions $(s_1, a_1, s_2, a_2, \dots)$, known as a trajectory.
 115

116 The policy is improved by ascending the gradient of this objective, $\nabla_\theta J(\theta)$. The foundational policy
 117 gradient theorem provides a way for the gradient computation:
 118

$$119 \quad \nabla_\theta J(\theta) = \mathbb{E}_{\tau \sim \pi_\theta} \left[\left(\sum_{t=1}^T \nabla_\theta \log \pi_\theta(a_t | s_t) \right) \left(\sum_{t=1}^T r(s_t, a_t) \right) \right], \quad (3)$$

121 where $\nabla_\theta \log \pi_\theta(a_t | s_t)$ indicates the direction in the parameter space that would be used to update
 122 the policy π_θ . This direction is then weighted by the sum of all rewards in the trajectory, effectively
 123 reinforcing action sequences that lead to higher overall rewards.
 124

125 3 METHODOLOGY

127 We introduce the One-Token Rollout algorithm, a novel fine-tuning method that adapts the principles
 128 of Policy Gradient to the token level. OTR reframes the standard fine-tuning process by treating each
 129 individual token generation step as a complete, single-step trajectory. This conceptual shift allows us
 130 to simplify the general policy gradient framework into a highly efficient, token-level reinforcement
 131 learning algorithm, where the supervised training data is repurposed to provide a reward signal.
 132

133 3.1 FROM POLICY GRADIENT TO ONE-TOKEN ROLLOUT

135 Our starting point is the foundational policy gradient theorem introduced in the Section 2. The core
 136 innovation of OTR is to consider the generation of a single token from a state s_t to an action a_t as
 137 a complete trajectory of length one. In this micro-trajectory, the summations over timesteps present
 138 in Equation (3) collapse, as there is only a single state-action pair. Consequently, the summations
 139 of $\nabla_\theta \log \pi_\theta(a_t | s_t)$ and $r(s_t, a_t)$ over T tokens in the original formula both reduce to terms for an
 140 individual token, and sampling a full trajectory τ simplifies to sampling a single action a_t from the
 141 policy $\pi_\theta(\cdot | s_t)$. The policy gradient for this single step thus simplifies dramatically to:
 142

$$143 \quad \nabla_\theta J(\theta) = \mathbb{E}_{a_t \sim \pi_\theta(\cdot | s_t)} [\nabla_\theta \log \pi_\theta(a_t | s_t) \cdot r(s_t, a_t)]. \quad (4)$$

144 To implement this, we approximate the expectation $\mathbb{E}[\cdot]$ using Monte Carlo estimation. At each
 145 timestep t of the original sequence, we perform a “rollout” by sampling multiple candidate actions
 146 from the current policy. This transforms the optimization problem into a practical, sample-based
 147 loss function.
 148

149 3.2 TOKEN-LEVEL ROLLOUT AND ON-POLICY REWARD

150 To facilitate the rollout, we first define a stochastic sampling policy and a reward mechanism.
 151

152 **Stochastic Policy for Exploration.** For a given state s_t , the LLMs first compute a vector of raw,
 153 unnormalized scores for every token in the vocabulary V . These scores are known as logits. Let
 154 l_a denote the logit corresponding to a specific action a . The model’s base policy, π_θ , is typically
 155 derived by applying the softmax function directly to these logits.
 156

157 To encourage exploration during the rollout, we create a new sampling policy, π'_θ , by introducing a
 158 temperature parameter κ . The sampling policy is defined as:
 159

$$160 \quad \pi'_\theta(a | s_t) = \text{softmax} \left(\frac{l_a}{\kappa} \right). \quad (5)$$

161 Consistent with its common use during model inference, the temperature adjusts the shape of the
 162 final probability distribution. We utilize a temperature $\kappa > 1$ to flatten the distribution, which
 163 increases the likelihood of sampling less probable tokens and thereby enhances exploration.
 164

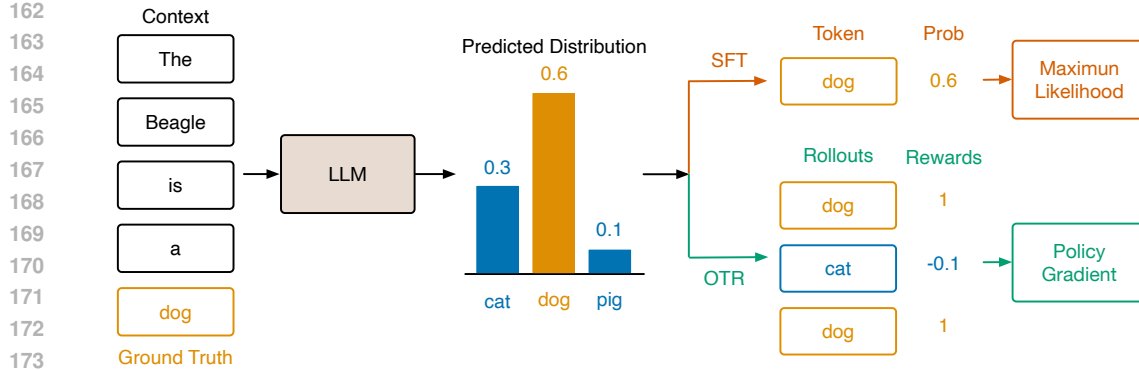


Figure 1: An illustration of the computational divergence between SFT and OTR.

Rollout and Reward Definition. At each timestep t , we draw a set of K candidate actions from our exploration policy:

$$\mathcal{A}'_t = \{a'_{t,j}\}_{j=1}^K, \quad \text{where each } a'_{t,j} \sim \pi'_\theta(\cdot|s_t). \quad (6)$$

Crucially, we use the ground-truth token x_t from the supervised dataset to construct an immediate reward signal. Each sampled action $a'_{t,j}$ is evaluated against x_t using the following reward function:

$$R(a'_{t,j}, x_t) = \begin{cases} 1 & \text{if } a'_{t,j} = x_t, \\ \beta & \text{if } a'_{t,j} \neq x_t. \end{cases} \quad (7)$$

Here, β is a hyperparameter where $\beta < 1$. A reward of 1 is given for “rediscovering” the ground-truth token, while a lesser reward β is given for all other tokens. We finally set $\beta = -0.1$ for our main experiments based on the ablation study detailed in Section 4.4.

This design elegantly converts the traditionally off-policy supervised data into an on-policy learning signal at the token level. The actions \mathcal{A}'_t we evaluate are sampled directly from the current policy π'_θ , and the fixed ground-truth token x_t is used simply to assign a real-time reward to these on-policy actions. This avoids the complexities of importance sampling or other off-policy correction techniques typically required in sentence-level RL.

3.3 THE OTR OBJECTIVE FUNCTION

Based on the token-level rollout and policy gradient in Equation (4), the loss at timestep t is the Monte Carlo approximation of the negative policy gradient objective, averaged over the K samples:

$$\mathcal{L}_{\text{OTR}}^t(\theta) = -\frac{1}{K} \sum_{j=1}^K [\text{sg}(R(a'_{t,j}, x_t)) \cdot \log \pi_\theta(a'_{t,j}|s_t)], \quad (8)$$

where π_θ is the model’s original, non-temperature-scaled policy, and $\text{sg}(\cdot)$ is the stop-gradient operator. Given our defined reward function, we can decompose this loss. Let $N_{gt} = \sum_{j=1}^K \mathbb{I}(a'_{t,j} = x_t)$ be the count of times the ground-truth token was sampled. The loss function simplifies to its final form:

$$\mathcal{L}_{\text{OTR}}^t(\theta) = -\frac{1}{K} \left[N_{gt} \log \pi_\theta(x_t|s_t) + \beta \sum_{j \text{ s.t. } a'_{t,j} \neq x_t} \log \pi_\theta(a'_{t,j}|s_t) \right]. \quad (9)$$

This per-timestep objective has an intuitive interpretation. The first term is a SFT-like loss for the ground-truth token, but it is dynamically weighted by its sampling frequency N_{gt} . If the ground-truth is never sampled, its loss contribution is zero. The second term acts as a regularizer, weighted by β , which penalizes the model for assigning high probability to the incorrect tokens it sampled.

The total loss for an entire sequence of length T is the average of these per-timestep losses:

$$\mathcal{L}_{\text{OTR}}(\theta) = \frac{1}{T} \sum_{t=1}^T \mathcal{L}_{\text{OTR}}^t(\theta). \quad (10)$$

216 This objective allows OTR to focus its optimization effort, reinforcing correct predictions that are
 217 already within the model’s reach while gently suppressing plausible alternatives, creating a more
 218 nuanced and effective learning signal than SFT alone. To visually summarize the computational
 219 divergence of the OTR update from the standard SFT, we provide a detailed illustration in Figure 1.
 220

221 **3.4 COMPARISON WITH DYNAMIC FINE-TUNING**
 222

223 Our work is related to the concurrent dynamic fine-tuning (DFT) method (Wu et al., 2025c), which
 224 also seeks to improve the generalization of SFT from a reinforcement learning perspective. DFT’s
 225 motivation stems from the insight that the standard SFT gradient contains an implicit, problematic
 226 inverse-probability weighting ($1/\pi_\theta$) that leads to optimization instability. To address this, DFT
 227 proposes to “rectify” the reward by reweighting the loss for the ground-truth token x_t with its own
 228 model probability $\pi_\theta(x_t|s_t)$. The resulting per-timestep DFT loss is:

$$\mathcal{L}_{\text{DFT}}^t(\theta) = -\text{sg}(\pi_\theta(x_t|s_t)) \log \pi_\theta(x_t|s_t). \quad (11)$$

229 The OTR framework can be seen as a generalization of DFT. This relationship becomes clear when
 230 we consider the special case of our OTR objective where the hyperparameter $\beta = 0$. In this scenario,
 231 the second term in Equation (9), which penalizes incorrect samples, vanishes. Then the OTR loss
 232 can be formulated as:

$$\mathcal{L}_{\text{OTR}}^t(\theta)|_{\beta=0} = -\frac{N_{gt}}{K} \log \pi_\theta(x_t|s_t), \quad (12)$$

233 where N_{gt}/K represents the empirical frequency of sampling the ground-truth token during the
 234 rollout. This frequency is a direct Monte Carlo approximation of the ground-truth token’s probability,
 235 i.e., $\frac{N_{gt}}{K} \approx \pi_\theta(x_t|s_t)$. Thus, when $\beta = 0$, the OTR objective is functionally equivalent to the DFT
 236 objective, as both methods effectively weight the loss of the ground-truth token by its estimated
 237 probability.

238 However, when $\beta \neq 0$, OTR extends beyond DFT’s formulation. In addition to reinforcing the
 239 “rediscovered” ground-truth token, OTR’s objective incorporates a crucial second term: a regular-
 240 ization penalty applied to the incorrect tokens sampled during the rollout. This allows OTR to not
 241 only learn from the positive signal of the ground-truth but also to actively discourage the model from
 242 assigning high probability to plausible but incorrect alternatives. Therefore, OTR provides a more
 243 comprehensive learning signal by leveraging information from both successful and unsuccessful
 244 samples within the model’s own distribution.

245 **4 EXPERIMENTS**
 246

247 **4.1 EXPERIMENT SETTINGS**
 248

249 **Dataset and Models.** We conduct experiments on the OpenR1-Math-220k dataset (OpenR1 Team,
 250 2025), which consists of 220,000 mathematical problems with detailed reasoning traces. These
 251 traces are generated by the DeepSeek R1 model (DeepSeek-AI et al., 2025) for problems originating
 252 from the NuminaMath-1.5 dataset (LI et al., 2024). To efficiently manage computational resources
 253 while ensuring data quality, we randomly sample a subset of 5,000 instances for our training set.
 254 All selected instances have reasoning traces with lengths under 8192 tokens, and their lengths are
 255 approximately uniformly distributed across different intervals. We utilize a suite of powerful and
 256 contemporary open-source LLMs as base models. Specifically, we conduct our experiments on the
 257 following models: Qwen2.5-3B (Qwen Team, 2024), Qwen2.5-7B (Qwen Team, 2024), Qwen3-4B-
 258 Base (Qwen Team, 2025), and Qwen3-8B-Base (Qwen Team, 2025).

259 **Training Details.** Our implementation is built upon the Verl framework, and to ensure a fair com-
 260 parison, both our proposed OTR algorithm and the SFT baseline are trained using identical settings.
 261 We employ the AdamW optimizer with a learning rate of 5×10^{-6} . The learning rate follows a
 262 cosine decay schedule, which includes a warm-up ratio of 0.03 and decays to 1×10^{-6} . For the
 263 training configuration, we use a batch size of 64 and a maximum sequence length of 10240 tokens.
 264 All models are trained for a total of 2 epochs.

270
 271 Table 1: Main results on in-domain mathematical reasoning benchmarks. For each model, the best
 272 result between SFT and OTR is in **bold**. The \dagger symbol indicates performance degradation compared
 273 to the base model.

Model	Method	GSM8K	MATH	Olympiad	Minerva	AIME24	AIME25	AMC23	Average
Qwen2.5-3B	Base	77.90	42.64	25.20	23.20	3.30	0.00	40.00	30.32
	SFT	82.05	62.50	26.23	24.90	7.30	1.65	37.03 \dagger	34.52
	OTR	82.93	63.95	27.05	25.00	7.71	2.91	40.78	35.76
Qwen2.5-7B	Base	85.36	49.80	36.40	28.30	6.70	3.30	42.50	36.05
	SFT	88.18	67.75	31.53 \dagger	32.53	8.54	5.00	43.75	39.61
	OTR	89.77	70.45	35.33\dagger	33.45	8.33	6.87	44.38	41.23
Qwen3-4B	Base	86.90	54.10	38.20	29.80	3.30	6.70	55.00	39.14
	SFT	74.13 \dagger	63.95	32.10 \dagger	29.60 \dagger	10.21	6.24 \dagger	42.66 \dagger	36.98 \dagger
	OTR	91.98	75.30	40.63	36.68	10.22	11.67	52.81\dagger	45.61
Qwen3-8B	Base	90.40	60.80	40.90	34.20	13.30	16.70	62.50	45.54
	SFT	83.77 \dagger	77.40	41.70	37.70	15.20	15.63\dagger	55.16 \dagger	46.65
	OTR	91.63	79.45	42.43	39.35	14.80	14.17 \dagger	59.53\dagger	48.77

287
 288 Table 2: Out-of-domain performance on code generation and general reasoning benchmarks. For
 289 each model, the best result between SFT and OTR is in **bold**. The \dagger symbol indicates performance
 290 degradation compared to the base model.

Model	Method	Code			General Reasoning			
		HumanEval+	MBPP+	Avg	BBEH	SuperGPQA	MMLU-Pro	Average
Qwen2.5-3B	Base	35.40	50.30	42.85	6.00	19.28	33.90	19.73
	SFT	57.60	48.20 \dagger	52.90	7.23	18.67 \dagger	36.15	20.68
	OTR	59.30	49.90\dagger	54.60	7.88	19.22\dagger	36.20	21.10
Qwen2.5-7B	Base	48.80	64.00	56.40	6.88	23.93	42.31	24.37
	SFT	68.50	58.10 \dagger	63.30	10.44	26.25	51.24	29.31
	OTR	69.00	59.20\dagger	64.10	11.28	26.32	51.22	29.61
Qwen3-4B	Base	56.70	62.40	59.55	8.19	28.56	53.35	30.03
	SFT	70.20	60.90 \dagger	65.55	9.27	28.11 \dagger	53.86	30.41
	OTR	74.00	62.90	68.45	9.71	29.03	55.96	31.57
Qwen3-8B	Base	61.60	63.50	62.55	9.91	32.53	59.57	34.00
	SFT	76.00	65.40	70.70	10.40	29.03 \dagger	53.82 \dagger	31.08 \dagger
	OTR	77.70	66.50	72.10	10.02	30.49\dagger	56.87\dagger	32.46\dagger

4.2 EVALUATION

306
 307 Our evaluation is designed to accurately reflect the impact of the SFT and OTR fine-tuning algo-
 308 rithms on the base models’ capabilities. To this end, we utilize a suite of challenging benchmarks
 309 spanning mathematical, code, and general reasoning domains to test the generalization of the
 310 algorithms, and we employ distinct evaluation settings for the base and fine-tuned models. For all
 311 evaluations, the maximum generation length is set to 8192 tokens.

312
 313 **Benchmarks and Metrics.** Our evaluation covers a suite of challenging benchmarks across three
 314 domains. For **mathematical reasoning**, our evaluation includes Minerva Math (Lewkowycz et al.,
 315 2022), MATH-500 (Hendrycks et al., 2021), GSM8K (Cobbe et al., 2021), OlympiadBench (He
 316 et al., 2024), AMC 2023, AIME 2024, and AIME 2025. For the highly challenging AMC 2023,
 317 AIME 2024, and AIME 2025 benchmarks, we report **mean@16** accuracy, while for the remaining
 318 math benchmarks, we report **mean@4** accuracy. For **code generation**, we use HumanEval Plus (Liu
 319 et al., 2023) and MBPP Plus (Liu et al., 2023), with performance measured by the **pass@1** metric.
 320 Finally, for **general domain reasoning**, we evaluate on MMLU-Pro (Wang et al., 2024), SuperG
 321 PQA (Du et al., 2025a), and BBEH (Kazemi et al., 2025) using **Exact Match (EM)** accuracy.

322
 323 **Base Model Evaluation.** To align with standard evaluation practices for base models, we use a
 324 natural prompt template for testing. Specifically, we employ a 5-shot setting for the MATH-500 and

324 Table 3: Ablation study on the hyperparameter β for in-domain mathematical reasoning.
325

Model	Method		GSM8K	MATH	Olympiad	Minerva	AIME24	AIME25	AMC23	Average
Qwen2.5-3B	OTR	SFT	82.05	62.50	26.23	24.90	7.30	1.65	37.03	34.52
		$\beta = \begin{cases} -1.00 \\ -0.10 \\ 0.00 \\ 0.01 \end{cases}$	83.10	63.05	26.05	25.75	6.88	2.91	37.66	35.06
			82.93	63.95	27.05	25.00	7.71	2.91	40.78	35.76
			83.65	63.10	27.48	22.35	8.34	2.69	39.53	35.31
Qwen3-4B	OTR	SFT	74.13	63.95	32.10	29.60	10.21	6.24	42.66	36.98
		$\beta = \begin{cases} -1.00 \\ -0.10 \\ 0.00 \\ 0.01 \end{cases}$	92.15	77.75	40.60	35.68	12.09	13.33	53.75	46.48
			91.98	75.30	40.63	36.68	10.22	11.67	52.81	45.61
			91.03	76.30	40.75	36.88	10.20	10.63	53.28	45.58
			90.15	76.30	39.35	36.95	9.79	9.79	51.41	44.82

335
336 GSM8K benchmarks and use a greedy sampling strategy with a temperature of 0 for decoding for
337 all benchmarks.
338

339 **Fine-tuned Model Evaluation.** For the chat models fine-tuned with SFT and OTR, we use their
340 respective chat templates and a 0-shot setting across all benchmarks. The decoding strategy is
341 stochastic sampling with a temperature of 0.7 and a top-p of 0.8.
342

343 4.3 RESULTS

344
345 We present the main experimental results in Table 1 for in-domain generalization and Table 2 for
346 out-of-domain (OOD) generalization. For all OTR experiments presented in this section, we set the
347 key hyperparameters for our algorithm: the temperature parameter $\kappa = 1.3$, the number of rollout
348 candidates $K = 256$, and the reward hyperparameter $\beta = -0.1$. The value for β was determined to
349 yield the best overall performance based on our ablation studies detailed in Section 4.4.
350

351 **In-Domain Generalization.** As shown in Table 1, OTR consistently demonstrates superior performance
352 over SFT on mathematical reasoning tasks. Across all four model families, OTR achieves a
353 higher average score. This highlights OTR’s effectiveness in enhancing the specialized capabilities
354 of the models within their training domain.
355

356 Furthermore, OTR shows greater generalization by mitigating the catastrophic forgetting often ob-
357 served during fine-tuning. The number of instances where performance degrades below the base
358 model (marked by the \dagger symbol) is significantly lower for OTR (4 instances) compared to SFT (10
359 instances). Even in cases where both methods underperform, OTR’s performance drop is consider-
360 ably milder. For example, on the AMC23 benchmark with Qwen3-8B, SFT’s score drops by 7.34
361 points relative to the base model, whereas OTR’s score drops by only 2.97 points. This suggests that
362 OTR’s on-policy signal helps preserve the valuable knowledge learned during pre-training.
363

364 **Out-of-Domain Generalization.** The advantages of OTR extend to out-of-domain tasks, as detailed
365 in Table 2. On both code generation and general reasoning benchmarks, OTR consistently surpasses
366 SFT in average performance across all models. This trend demonstrates that OTR effectively lever-
367 ages its on-policy signal to achieve broader, more generalized capabilities that are not confined to
368 its training domain.
369

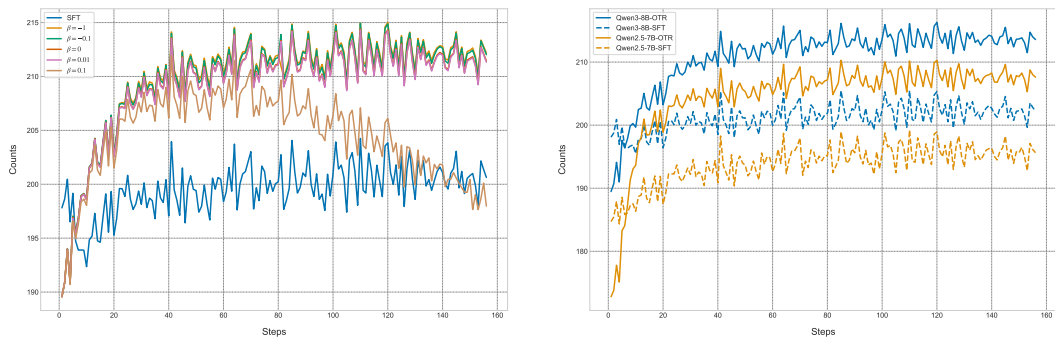
370 From the perspective of knowledge preservation, OTR again proves to be a more generalizable algo-
371 rithm. SFT underperforms its base model in 7 OOD instances, particularly showing vulnerability on
372 SuperGPQA and MMLU-Pro with larger models. In contrast, OTR underperforms in 5 instances and
373 shows consistent improvements on general reasoning for the Qwen3-4B model where SFT struggles.
374 This demonstrates that OTR provides a more reliable fine-tuning approach that not only enhances
375 target skills but also better maintains the model’s general intelligence, leading to superior overall
376 generalization. A supplementary experiment is detailed in Appendix A.
377

378 4.4 ABLATION STUDY

379 To investigate the impact of the reward hyperparameter β , we conduct a comprehensive ablation
380 study. We select four values for analysis, ranging from negative to positive: -1.0, -0.1, 0, and
381 0.01. The performance across in-domain and out-of-domain benchmarks is presented in Table 3
382

378 Table 4: Ablation study on the hyperparameter β for out-of-domain generalization.
379

380 Model	381 Method	382 Code			383 General Tasks			
		384 HumanEval+	385 MBPP+	386 Avg	387 BBEH	388 SuperGPQA	389 MMLU-Pro	390 Average
382	383 SFT	384 57.60	385 48.20	386 52.90	387 7.23	388 18.67	389 36.15	390 20.68
383 Qwen2.5-3B	384 $\beta = \begin{cases} -1.00 \\ -0.10 \\ 0.00 \\ 0.01 \end{cases}$	385 57.90	386 49.70	387 53.80	388 7.28	389 19.07	390 36.26	391 20.87
		385 59.30	386 49.90	387 54.60	388 7.88	389 19.22	390 36.20	391 21.10
		385 58.90	386 49.20	387 54.05	388 8.38	389 19.39	390 36.16	391 21.31
		385 60.50	386 49.90	387 55.20	388 7.59	389 19.08	390 36.49	391 21.05
382	383 SFT	384 70.20	385 60.90	386 65.55	387 9.27	388 28.11	389 53.86	390 30.41
383 Qwen3-4B	384 $\beta = \begin{cases} -1.00 \\ -0.10 \\ 0.00 \\ 0.01 \end{cases}$	385 74.20	386 61.10	387 67.65	388 9.91	389 28.65	390 56.51	391 31.69
		385 74.00	386 62.90	387 68.45	388 9.71	389 29.03	390 55.96	391 31.57
		385 73.70	386 61.90	387 67.80	388 9.54	389 28.24	390 53.93	391 30.57
		385 73.20	386 62.20	387 67.70	388 8.38	389 26.11	390 50.37	391 28.29

402 Figure 2: Analysis of the number of GT tokens sampled during training. (a) Compares OTR with
403 different β values against SFT on Qwen3-4B. (b) Compares OTR and SFT on larger models.
404

408 and Table 4, respectively. To provide insight into the training process for our subsequent analysis,
409 we also track a key diagnostic metric: the number of ground-truth (GT) tokens sampled during the
410 token-level rollout. For a direct comparison, we also record this metric for SFT. It is important to
411 note that this measurement is for analysis only and does not alter the standard SFT algorithm.

412 **Effect of β on Training Stability.** Our first key observation relates to training stability, as depicted
413 in Figure 2(a). While most OTR variants show a stable increase in GT token counts, the setting with
414 $\beta = 0.1$ exhibits clear training instability. Its GT count initially rises but then collapses in the later
415 stages. We hypothesize that assigning a positive reward to incorrectly sampled tokens, especially
416 a relatively high one, can mislead the optimization process. This may cause the model to increase
417 the probabilities of all rolled-out tokens indiscriminately, ultimately leading to a degradation of the
418 learned distribution. This observed instability motivates us to limit our search space, leading to our
419 selection of β values $\{-1.0, -0.1, 0, 0.01\}$, which primarily explores the non-positive range.

420 **Impact on Performance and Optimal β Selection.** From the performance results in Table 3 and Ta-
421 ble 4, it is evident that OTR is robustly superior to SFT. Regardless of the specific β value, OTR
422 variants consistently outperform the SFT baseline in terms of average scores across nearly all do-
423 mains and models. Among these variants, the setting of $\beta = -0.1$ demonstrates the most consistent
424 and high-level performance across both in-domain and OOD tasks. Therefore, we select $\beta = -0.1$
425 as the default value for our main experiments.

426 **The Importance of Negative Samples.** This study also provides insight into the importance of
427 utilizing negative samples. As analyzed in Section 3.4, OTR with $\beta = 0$ can be viewed as a Monte
428 Carlo approximation of the DFT method. A direct comparison between the $\beta = -0.1$ and $\beta = 0$
429 rows in our tables reveals that the former almost universally outperforms the latter. This result
430 provides empirical evidence that incorporating an explicit penalty for negatively sampled tokens is
431 a crucial component of OTR’s success, contributing to a more effective learning signal than what is
offered by SFT-like formulations.

432 **Analysis of Learning Dynamics.** Finally, we analyze the source of OTR’s general superiority over
 433 SFT by examining the GT token counts at convergence in Figure 2. Across different models, scales,
 434 and architectures (as shown in both Figure 2(a) and Figure 2(b)), OTR-trained models consistently
 435 converge to a higher number of sampled GT tokens than SFT-trained models. A higher GT count
 436 indicates that the model’s learned policy assigns a higher probability to the ground-truth sequences,
 437 which suggests a lower perplexity on the training data. We infer from this that OTR enables the
 438 model to learn from and utilize the training data more profoundly and efficiently than SFT, poten-
 439 tially unlocking a higher performance ceiling.

440

441 5 RELATED WORK

442

443 **Reinforcement Learning for Language Models.** Recently, reinforcement learning has gained
 444 significant traction as a powerful paradigm for enhancing the capabilities of large language mod-
 445 els (Hu, 2025; DeepSeek-AI et al., 2025; Wu et al., 2025a). The success of state-of-the-art models,
 446 which have leveraged RL-based algorithms like GRPO (Shao et al., 2024) to achieve substantial im-
 447 provements in reasoning and cross-domain generalization, has catalyzed a surge of interest in these
 448 methods. The traditional approach to RL fine-tuning, reinforcement learning from human feedback
 449 (RLHF) (Ouyang et al., 2022), often relies on complex and computationally intensive algorithms
 450 like PPO (Schulman et al., 2017). The inherent instability and implementation complexity of PPO
 451 have motivated a recent wave of research focused on simplifying the RLHF pipeline. A prominent
 452 line of work, including methods like DPO (Rafailov et al., 2023) and GEPO (Wu et al., 2025b), ele-
 453 gantly reframes the preference learning objective to create a simple loss, eliminating the need for an
 454 explicit reward model. In a similar spirit, GPG (Chu et al., 2025b) simplifies the RL objective into
 455 a weighted maximum likelihood form, demonstrating that such a simplified approach can match the
 456 performance of more complex algorithms.

457 **Improving Supervised Fine-tuning.** While SFT is the most widely used paradigm for fine-tuning,
 458 its limitations, such as catastrophic forgetting and deviation from the pre-trained model’s distribu-
 459 tion, are well-documented (Kumar et al., 2022; Huan et al., 2025). A major line of research aims
 460 to improve SFT by modifying its objective function. A prominent example is proximal SFT (Zhu
 461 et al., 2025), which introduces a proximal regularization term to the SFT loss to penalize divergence
 462 from the initial model’s policy. This approach is analogous to the KL-divergence constraint in PPO
 463 and helps stabilize training and preserve pre-trained knowledge. Another significant line of work
 464 seeks to enhance SFT by reformulating it through the lens of reinforcement learning, often by es-
 465 tablishing a mathematical connection between their objectives. For instance, some studies reframe
 466 RLHF as a reward-weighted form of SFT (Du et al., 2025b), while others view SFT as an RL method
 467 with an implicit reward function (Wang et al., 2025; Qin & Springenberg, 2025). Concurrent to our
 468 work, DFT (Wu et al., 2025c) identifies an implicit inverse-probability weighting in the SFT gradi-
 469 ent and addresses the resulting instability by re-weighting the loss for the ground-truth token with
 470 its own model probability. Although these works build a theoretical bridge between SFT and RL,
 471 they primarily focus on re-weighting the loss for the static, ground-truth expert data. In contrast,
 472 our work offers a distinct, data-centric solution. OTR moves beyond loss modification and instead
 473 transforms the training data itself into a dynamic, on-policy signal by actively sampling from the
 474 model’s current policy.

475

6 CONCLUSION

476

477 In this work, we investigated the generalization weakness of SFT compared to RL, positing that
 478 the disparity stems from the fundamental difference between SFT’s static, off-policy data and RL’s
 479 dynamic, on-policy data. To bridge this gap from a data-centric perspective, we introduced One-
 480 Token Rollout, a novel fine-tuning algorithm. By reframing each token generation as a single-
 481 step reinforcement learning trajectory, OTR transforms the static supervised dataset into a dynamic,
 482 on-policy learning signal, successfully incorporating the advantage of on-policy data into the SFT
 483 framework while maintaining its computational efficiency. Our extensive experiments empirically
 484 validate this approach, demonstrating that OTR consistently outperforms SFT on a wide array of
 485 in-domain and out-of-domain benchmarks. Ultimately, we present OTR as a powerful and practical
 486 alternative for fine-tuning LLMs, providing compelling evidence that simulating on-policy interac-
 487 tion is a key direction for developing more generalizable fine-tuned language models.

486 REFERENCES
487

488 Tianzhe Chu, Yuexiang Zhai, Jihan Yang, Shengbang Tong, Saining Xie, Dale Schuurmans, Quoc V
489 Le, Sergey Levine, and Yi Ma. Sft memorizes, rl generalizes: A comparative study of foundation
490 model post-training. *arXiv preprint arXiv:2501.17161*, 2025a.

491 Xiangxiang Chu, Hailang Huang, Xiao Zhang, Fei Wei, and Yong Wang. GPG: A Simple and
492 Strong Reinforcement Learning Baseline for Model Reasoning. *arXiv preprint arXiv:2504.02546*,
493 2025b.

494 Hyung Won Chung, Le Hou, Shayne Longpre, Barret Zoph, Yi Tay, William Fedus, Yunxuan
495 Li, Xuezhi Wang, Mostafa Dehghani, Siddhartha Brahma, Albert Webson, Shixiang Shane Gu,
496 Zhuyun Dai, Mirac Suzgun, Xinyun Chen, Aakanksha Chowdhery, Alex Castro-Ros, Marie Pel-
497 lat, Kevin Robinson, Dasha Valter, Sharan Narang, Gaurav Mishra, Adams Yu, Vincent Zhao,
498 Yanping Huang, Andrew Dai, Hongkun Yu, Slav Petrov, Ed H. Chi, Jeff Dean, Jacob Devlin,
499 Adam Roberts, Denny Zhou, Quoc V. Le, and Jason Wei. Scaling Instruction-Finetuned Lan-
500 guage Models. *arXiv preprint arXiv:2210.11416*, 2022.

501 Karl Cobbe, Vineet Kosaraju, Mohammad Bavarian, Mark Chen, Heewoo Jun, Lukasz Kaiser,
502 Matthias Plappert, Jerry Tworek, Jacob Hilton, Reiichiro Nakano, et al. Training verifiers to
503 solve math word problems. *arXiv preprint arXiv:2110.14168*, 2021.

504 DeepSeek-AI, Daya Guo, Dejian Yang, Haowei Zhang, Junxiao Song, Ruoyu Zhang, Runxin Xu,
505 Qihao Zhu, Shirong Ma, Peiyi Wang, et al. DeepSeek-R1: Incentivizing Reasoning Capability in
506 LLMs via Reinforcement Learning. *arXiv preprint arXiv:2501.12948*, 2025.

507 Xinrun Du, Yifan Yao, Kaijing Ma, Bingli Wang, Tianyu Zheng, King Zhu, Minghao Liu, Yiming
508 Liang, Xiaolong Jin, Zhenlin Wei, et al. Supergpqa: Scaling llm evaluation across 285 graduate
509 disciplines. *arXiv preprint arXiv:2502.14739*, 2025a.

510 Yuhao Du, Zhuo Li, Pengyu Cheng, Zhihong Chen, Yuejiao Xie, Xiang Wan, and Anningzhe Gao.
511 Simplify rlhf as reward-weighted sft: A variational method. *arXiv preprint arXiv:2502.11026*,
512 2025b.

513 Chaoqun He, Renjie Luo, Yuzhuo Bai, Shengding Hu, Zhen Leng Thai, Junhao Shen, Jinyi Hu,
514 Xu Han, Yujie Huang, Yuxiang Zhang, et al. Olympiadbench: A challenging benchmark for
515 promoting agi with olympiad-level bilingual multimodal scientific problems. *arXiv preprint
arXiv:2402.14008*, 2024.

516 Dan Hendrycks, Collin Burns, Saurav Kadavath, Akul Arora, Steven Basart, Eric Tang, Dawn Song,
517 and Jacob Steinhardt. Measuring mathematical problem solving with the math dataset. *arXiv
preprint arXiv:2103.03874*, 2021.

518 Jian Hu. Reinforce++: A simple and efficient approach for aligning large language models. *arXiv
preprint arXiv:2501.03262*, 2025.

519 Maggie Huan, Yuetai Li, Tuney Zheng, Xiaoyu Xu, Seungone Kim, Minxin Du, Radha Poovendran,
520 Graham Neubig, and Xiang Yue. Does Math Reasoning Improve General LLM Capabilities?
521 Understanding Transferability of LLM Reasoning. *arXiv preprint arXiv:2507.00432*, 2025.

522 Mehran Kazemi, Bahare Fatemi, Hritik Bansal, John Palowitch, Chrysovalantis Anastasiou, San-
523 ket Vaibhav Mehta, Lalit K Jain, Virginia Aglietti, Disha Jindal, Peter Chen, et al. Big-bench
524 extra hard. *arXiv preprint arXiv:2502.19187*, 2025.

525 Ananya Kumar, Aditi Raghunathan, Robbie Jones, Tengyu Ma, and Percy Liang. Fine-
526 tuning can distort pretrained features and underperform out-of-distribution. *arXiv preprint
arXiv:2202.10054*, 2022.

527 Aitor Lewkowycz, Anders Andreassen, David Dohan, Ethan Dyer, Henryk Michalewski, Vinay Ra-
528 masesh, Ambrose Slone, Cem Anil, Imanol Schlag, Theo Gutman-Solo, et al. Solving quantitative
529 reasoning problems with language models. *Advances in neural information processing systems*,
530 2022.

540 Jia LI, Edward Beeching, Lewis Tunstall, Ben Lipkin, Roman Soletskyi, Shengyi Costa Huang,
 541 Kashif Rasul, Longhui Yu, Albert Jiang, Ziju Shen, Zihan Qin, Bin Dong, Li Zhou, Yann
 542 Fleureau, Guillaume Lample, and Stanislas Polu. NuminaMath. [<https://huggingface.co/AI-MO/NuminaMath-CoT>] (https://github.com/project-numina/aimo-progress-prize/blob/main/report/numina_dataset.pdf), 2024.

543

544

545 Jiawei Liu, Chunqiu Steven Xia, Yuyao Wang, and Lingming Zhang. Is Your Code Generated by
 546 ChatGPT Really Correct? Rigorous Evaluation of Large Language Models for Code Generation.
 547 In *Thirty-seventh Conference on Neural Information Processing Systems*, 2023.

548

549 OpenR1 Team. OpenR1-Math-220k. <https://huggingface.co/datasets/open-r1/OpenR1-Math-220k>, 2025.

550

551 Long Ouyang, Jeff Wu, Xu Jiang, Diogo Almeida, Carroll L. Wainwright, Pamela Mishkin, Chong
 552 Zhang, Sandhini Agarwal, Katarina Slama, Alex Ray, John Schulman, Jacob Hilton, Fraser Kel-
 553 ton, Luke Miller, Maddie Simens, Amanda Askell, Peter Welinder, Paul Christiano, Jan Leike,
 554 and Ryan Lowe. Training language models to follow instructions with human feedback. *arXiv*
 555 preprint [arXiv:2203.02155](https://arxiv.org/abs/2203.02155), 2022.

556

557 Chongli Qin and Jost Tobias Springenberg. Supervised fine tuning on curated data is reinforcement
 558 learning (and can be improved). *arXiv preprint arXiv:2507.12856*, 2025.

559

560 Qwen Team. Qwen2.5: A party of foundation models. September 2024. URL <https://qwenlm.github.io/blog/qwen2.5/>.

561

562 Qwen Team. Qwen3 technical report. 2025. URL <https://arxiv.org/abs/2505.09388>.

563

564 Rafael Rafailov, Archit Sharma, Eric Mitchell, Christopher D Manning, Stefano Ermon, and Chelsea
 565 Finn. Direct preference optimization: Your language model is secretly a reward model. *Advances*
 566 in *neural information processing systems*, 2023.

567

568 Yi Ren and Danica J Sutherland. Learning dynamics of llm finetuning. *arXiv preprint*
 569 [arXiv:2407.10490](https://arxiv.org/abs/2407.10490), 2024.

570

571 John Schulman, Filip Wolski, Prafulla Dhariwal, Alec Radford, and Oleg Klimov. Proximal Policy
 572 Optimization Algorithms. *arXiv preprint arXiv:1707.06347*, 2017.

573

574 Zhihong Shao, Peiyi Wang, Qihao Zhu, Runxin Xu, Junxiao Song, Xiao Bi, Haowei Zhang,
 575 Mingchuan Zhang, Y. K. Li, Y. Wu, and Daya Guo. DeepSeekMath: Pushing the Limits of
 576 Mathematical Reasoning in Open Language Models. *arXiv preprint arXiv:2402.03300*, 2024.

577

578 Idan Shenfeld, Jyothish Pari, and Pulkit Agrawal. RL's Razor: Why Online Reinforcement Learning
 579 Forgets Less. *arXiv preprint arXiv:2509.04259*, 2025.

580

581 Fahim Tajwar, Anikait Singh, Archit Sharma, Rafael Raffailov, Jeff Schneider, Tengyang Xie, Stefano
 582 Ermon, Chelsea Finn, and Aviral Kumar. Preference fine-tuning of llms should leverage
 583 suboptimal, on-policy data. *arXiv preprint arXiv:2404.14367*, 2024.

584

585 Bo Wang, Qinyuan Cheng, Runyu Peng, Rong Bao, Peiji Li, Qipeng Guo, Linyang Li, Zhiyuan
 586 Zeng, Yunhua Zhou, and Xipeng Qiu. Implicit Reward as the Bridge: A Unified View of SFT and
 587 DPO Connections. *arXiv preprint arXiv:2507.00018*, 2025.

588

589 Yubo Wang, Xueguang Ma, Ge Zhang, Yuansheng Ni, Abhranil Chandra, Shiguang Guo, Weiming
 590 Ren, Aaran Arulraj, Xuan He, Ziyan Jiang, et al. Mmlu-pro: A more robust and challenging multi-
 591 task language understanding benchmark. *Advances in Neural Information Processing Systems*,
 592 2024.

593

594 Haoyuan Wu, Xueyi Chen, Rui Ming, Jilong Gao, Shoubo Hu, Zhuolun He, and Bei Yu. ToTRL:
 595 Unlock LLM Tree-of-Thoughts Reasoning Potential through Puzzles Solving. *arXiv preprint*
 596 [arXiv:2505.12717](https://arxiv.org/abs/2505.12717), 2025a.

597

598 Haoyuan Wu, Rui Ming, Jilong Gao, Hangyu Zhao, Xueyi Chen, Yikai Yang, Haisheng Zheng,
 599 Zhuolun He, and Bei Yu. On-Policy Optimization with Group Equivalent Preference for Multi-
 600 Programming Language Understanding. *arXiv preprint arXiv:2505.12723*, 2025b.

594 Yongliang Wu, Yizhou Zhou, Zhou Ziheng, Yingzhe Peng, Xinyu Ye, Xinting Hu, Wenbo Zhu,
595 Lu Qi, Ming-Hsuan Yang, and Xu Yang. On the Generalization of SFT: A Reinforcement Learn-
596 ing Perspective with Reward Rectification. *arXiv preprint arXiv:2508.05629*, 2025c.
597

598 Shengyu Zhang, Linfeng Dong, Xiaoya Li, Sen Zhang, Xiaofei Sun, Shuhe Wang, Jiwei Li, Runyi
599 Hu, Tianwei Zhang, Fei Wu, and Guoyin Wang. Instruction Tuning for Large Language Models:
600 A Survey. *arXiv preprint arXiv:2308.10792*, 2025.

601 Wenhong Zhu, Ruobing Xie, Rui Wang, Xingwu Sun, Di Wang, and Pengfei Liu. Proximal Super-
602 vised Fine-Tuning. *arXiv preprint arXiv:2508.17784*, 2025.

603

604

605

606

607

608

609

610

611

612

613

614

615

616

617

618

619

620

621

622

623

624

625

626

627

628

629

630

631

632

633

634

635

636

637

638

639

640

641

642

643

644

645

646

647

648 **A ADDITIONAL EXPERIMENT**
649650 To assess the robustness of our method and validate its generalization benefits across different
651 training data and training configurations, we conduct an additional experiment. For this analysis,
652 we adopt the training data and hyperparameter settings from the concurrent work, dynamic fine-
653 tuning (Wu et al., 2025c), which provides a distinct training environment to test the efficacy of OTR.
654 This comparative analysis focuses on the Qwen2.5-3B (Qwen Team, 2024) and Qwen3-4B (Qwen
655 Team, 2025) models, with the detailed setup provided below.656 **Dataset.** We train with the NuminaMath CoT dataset (LI et al., 2024), which comprises around
657 860,000 mathematical problems paired with corresponding solutions. To efficiently manage com-
658 putational resources, we randomly sample 50,000 instances from this dataset for training.
659660 **Training Details.** Our implementation is built upon the Verl framework. For a fair comparison, both
661 our proposed OTR algorithm and the SFT baseline are trained using identical settings. Specifically,
662 we employ the AdamW optimizer with a peak learning rate of 5×10^{-5} . The learning rate follows
663 a cosine decay schedule with a warm-up ratio of 0.1. We use a batch size of 256, a maximum input
664 length of 4096 tokens, and train all models for 1 epoch.665 As shown in Table 5, even under the training settings adapted from DFT, our OTR method con-
666 sistently outperforms the standard SFT baseline across the majority of benchmarks. This finding
667 demonstrates the robustness of the OTR algorithm and suggests that its generalization benefits are
668 not confined to a specific set of data and hyperparameters but hold true across different settings.669 Table 5: Results of SFT and OTR on in-domain math benchmarks when trained under the DFT
670 experimental settings. For each model, the best result is in **bold**.
671

Model	Method	GSM8K	MATH	Olympiad	Minerva	AIME24	AIME25	AMC23	Average
Qwen2.5-3B	SFT	78.50	53.25	19.43	16.55	2.28	0.83	24.53	27.91
	OTR	78.70	57.10	21.53	21.50	2.70	1.86	28.75	30.31
Qwen3-4B	SFT	88.75	64.80	30.60	27.30	6.25	4.38	35.78	36.84
	OTR	88.05	68.65	33.88	25.90	9.38	6.46	42.66	39.28

672
673 **LIMITATIONS**
674675 While our experiments demonstrate OTR’s consistent advantages across a range of models and
676 benchmarks, this work has several limitations. First, due to computational constraints, our study
677 is conducted on models up to 8 billion parameters and trained on a subset of a mathematics-focused
678 dataset. Consequently, the scalability of OTR to larger-scale models (e.g., 70B+) remains to be
679 validated. Second, our investigation is confined to the text-only modality. The reward mechanism,
680 while effective, is also relatively simple. Future work will aim to address these limitations by scaling
681 OTR to larger models, training on larger datasets, and extending it to broader training domains. We
682 also plan to explore more sophisticated reward functions, investigate the potential of multi-token
683 rollouts, and extend the OTR framework to other modalities, such as vision-language tasks.
684685 **DECLARATION OF LLM USAGE**
686687 The usage of LLMs is strictly limited to aid and polish the paper writing.
688689
690
691
692
693
694
695
696
697
698
699
700
701